Dissociative Ionization of H_2: A Study of Angular Distributions and Energy Distributions of Resultant Fast Protons*

GORDON H. DUNN AND L. J. KIEFFER
Joint Institute for Laboratory Astrophysics, Boulder, Colorado†
(Received 22 July 1963)

Protons with energies between 2 and 14 eV have been observed from dissociative ionization of H_2 using a rotatable collision chamber in conjunction with a small 60° sector magnetic spectrometer, and using electrons with energies ranging from threshold to 1500 eV. The degree of anisotropy in the angular distribution of protons is found to be dependent on electron energy. The anisotropy is analyzed in terms of selection rules and in terms of electron scattering using an analogy with dissociative excitation. The effects of the anisotropy and its electron energy dependence on measurements of cross sections and the energy distribution of protons is investigated. The energy distribution of protons is measured as a function of electron energy, and quite good agreement is found with predictions of the Franck–Condon principle. This is in rather sharp contrast with results of previous investigators.

I. INTRODUCTION

IT is interesting that in Bleakney's important paper[1] reporting the first observation of dissociative ionization of H_2 his introductory statement in 1930 was, "The ions produced by electron impact in hydrogen have been studied by the method of positive ray analysis so many times and by so many investigators that it might, at first sight, seem useless to try to make much more progress in this direction."

It might be thought that such a statment could be put even more forcefully today since, subsequently to Bleakney's work, many studies of this process have been reported. Lozier[2] and Newhall[3] investigated the energy distributions of the resultant fast protons and the relative cross sections for their formation. The proton energy distributions were also measured by Hagstrum and Tate,[4] Hagstrum,[5] and by Stevenson.[6] Bauer and Beach[7] and Schaefer and Hastings[8] studied isotopic effects in the relative probability of formation of protons from the $^2\Sigma_g^+$ state compared to formation of the bound ion in the $^2\Sigma_g^+$ state. Harrison[9] has measured the relative cross section for formation of protons. Sasaki and Nakao[10] observed the angular distribution of protons with energies between 5 and 9 eV formed by bombarding H_2 with electrons at approximately 100 eV.

Much similar work has also been done on other molecular species and other forms of dissociative collisions. Excellent reviews of this work have been published by Massey and Burhop[11] and by Craggs and Massey.[12]

In spite of the work since that of Bleakney, at least two important aspects of this process need further clarification and study. These are the subject of this paper.

The first concerns the angular distribution of resultant fast protons. The work of Sasaki and Nakao showed the angular distribution of the protons to be strongly peaked in the direction of the incident electron beam, but they did not investigate the electron energy dependence of this anisotropy. Neither they nor others have investigated or taken into account the effects of this anisotropy on measurements of relative cross sections and proton energy distributions.

Dunn[13] has pointed out that anisotropies such as were observed[10] and calculated[14] by Sasaki and Nakao, and calculated by Kerner,[15] can be expected for many dissociative transitions in all diatomic molecules. It is thus important to gain as much understanding as possible of such anisotropies with a simple molecule such as H_2.

This paper reports measurements of the angular distributions of protons from dissociative ionization of H_2 by electron impact over the electron energy range from threshold to 1500 eV. The effects of the anisotropy of the angular distribution of protons are discussed in some detail. The variation of angular distribution of protons with energy is discussed in terms of the electron scattering.

Stevenson[6] has pointed out that the measured energy distributions previously reported in the literature are inconsistent with the predictions of the Franck-Condon rule. This paper reports measurements of proton energy distributions which are consistent with the predictions

* This research was supported in part by the Controlled Thermonuclear Branch of the Atomic Energy Commission and by A. R. P. A. as part of Project Defender.
† National Bureau of Standards, University of Colorado.
[1] W. Bleakney, Phys. Rev. **35**, 1180 (1930).
[2] W. W. Lozier, Phys. Rev. **36**, 1285 (1930).
[3] H. F. Newhall, Phys. Rev. **62**, 11 (1942).
[4] H. D. Hagstrum and J. T. Tate, Phys. Rev. **59**, 354 (1941).
[5] H. D. Hagstrum, Rev. Mod. Phys. **23**, 185 (1951).
[6] D. P. Stevenson, J. Am. Chem. Soc. **82**, 5961 (1960).
[7] N. Bauer and J. Y. Beach, J. Chem. Phys. **15**, 150 (1947).
[8] O. A. Schaefer and J. M. Hastings, J. Chem. Phys. **18**, 1048 (1950).
[9] H. Harrison, Ph.D. thesis, Catholic University, Washington, D. C., 1956 (unpublished).
[10] N. Sasaki and T. Nakao, Proc. Imp. Acad. (Tokyo) **11**, 138 (1935); Proc. Imp. Acad. (Tokyo) **17**, 75 (1941).
[11] H. S. W. Massey and E. H. S. Burhop, *Electronic and Ionic Impact Phenomena* (Oxford University Press, London, 1956).
[12] J. D. Craggs and H. S. W. Massey, in *Encyclopedia of Physics*, edited by S. Flügge (Springer-Verlag, Berlin, 1959), Vol. 37, Part 1.
[13] G. H. Dunn, Phys. Rev. Letters **8**, 62 (1962).
[14] N. Sasaki and T. Nakao, Proc. Imp. Acad. (Tokyo) **11**, 413 (1935).
[15] E. H. Kerner, Phys. Rev. **92**, 1441 (1953).

of the Franck-Condon rule over an electron energy range from near threshold to 1500 eV.

II. EXPERIMENTAL

A. General

Figure 1 is a potential energy diagram for the ground state of H_2, some of the states of H_2^+, and H_2^{++}. Electrons colliding with H_2 in the ground state, $^1\Sigma_g^+$, may ionize the H_2 leaving the H_2^+ in the $^2\Sigma_g^+$ bound state, the $^2\Sigma_u^+$ dissociative state, or other higher dissociative states. Transitions to these higher states are relatively unlikely since they involve excitation of both electrons.[16] Dissociative ionization of H_2 thus primarily yields some protons from above the dissociation limit of the $^2\Sigma_g^+$ state of H_2^+ (i.e., at small internuclear separations) and from the $^2\Sigma_u^+$ state of H_2^+. The expected energy distributions of these protons is indicated on the left of Fig. 1 assuming no angular effects. The relative heights of these two curves are not to be compared.

Figure 2 shows schematically the geometry and components used in the experiment. The electron gun G was attached directly to a cylindrical scattering chamber S which could be rotated about its axis. Ions that are formed at the center of the scattering chamber by the electron beam drift out through a slot in the scattering chamber, through an aperture-tube system composed of L_1, L_2, L_3, L_4, and into a 60-deg-sector-field-magnetic spectrometer A. Ions of the appropriate momenta are focused on the exit slit E_1 after which they are accelerated by 1500 V onto the cathode of a magnetic electron multiplier M.

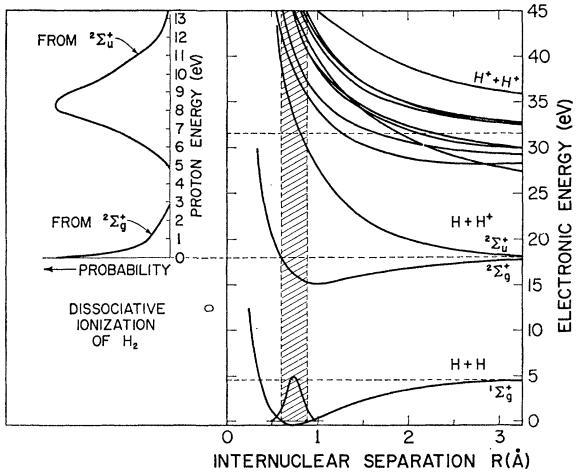

FIG. 1. Potential-energy diagram for the ground state of H_2, some of the states of H_2^+, and H_2^{++}. The energy scale is relative to the ground vibrational level of H_2. On the left is indicated the expected energy distributions of protons from the $^2\Sigma_g^+$ and $^2\Sigma_u^+$ states of H_2^+. The relative heights of these two curves are not to be compared.

[16] W. E. Lamb, Jr., and M. Skinner, Phys. Rev. **78**, 539 (1950).

The experiments performed were as follows:

(1) With a fixed electron energy E and fixed magnetic field in A ion currents were measured for different values of θ. This was repeated for ten values of E between 35 and 1500 eV and for magnetic fields in A which select protons of energies 3.7, 8.6, and 11.8 eV.

(2) For fixed values of E and θ the magnetic field in A was varied. The relative ion currents observed as a function of magnetic field thus represent the energy distribution of the protons formed (ϵ designates the proton energy). This was repeated for the values of E mentioned above and for several values of θ.

(3) For fixed values of θ and fixed fields in A the electron energy E was scanned. The relative ion currents as a function of E thus represent the relative cross section for formation of protons with a particular energy. This was repeated for several values of θ and magnetic field.

B. Details of Method and Apparatus

The entire experimental apparatus was contained in a glass bell jar vacuum system pumped by a 600 liter/sec liquid air-trapped mercury diffusion pump. Typical background pressures were $2-3\times10^{-7}$ Torr, as read on an Alpert-type ion gauge. Commercial hydrogen was leaked into the system through a needle valve and the leak rate adjusted until a pressure of about 4×10^{-5} Torr was read on the ion gauge. The diffusion pump worked continuously so that fresh gas was leaking in at all times during the experiment. The proton signals observed were linear with pressure over approximately three decades of pressure. Data were taken in approximately the middle of this pressure range. Impurity ions

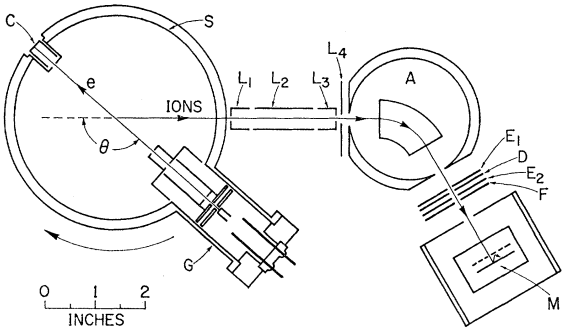

FIG. 2. Schematic drawing of the apparatus used in the experiment. The electron gun G is attached directly to the cylindrical scattering chamber S which can be rotated about its axis. C, the collecting cup for the electron beam, is also attached to the scattering chamber but is electrically isolated so that the electron beam current can be measured. Ions formed at the center of the scattering chamber drift out through a slot in S, through an aperture tube system, L_1, L_2, L_3, L_4 and into the spectrometer A. Ions of the appropriate momentum are focused on the exit slit E_1. Grid F is at a high negative potential which accelerates the positive ions to the dynode strip of the magnetic electron multiplier M. Grid E_2 is at the spectrometer potential. Grid D was usually at the spectrometer potential but under some conditions was at a positive potential relative to the spectrometer in order to prevent the thermal H_2^+ ions from entering the multiplier.

were monitored by accelerating the ions prior to their entry into A, and scanning the field in A. As might be expected in such a system, the major impurity ions were those of H_2O, O_2, and N_2. The currents observed from impurity ions were essentially constant over the large pressure range in which the proton signals were linear with pressure. It was thus concluded that secondary collisions and impurity gases do not contribute significantly to the observations.

The electron gun was designed to produce a parallel beam of electrons with divergence of less than 3°. Electrons from a barium impregnated tungsten cathode were focused through a 1 mm aperture with a Soa lens[17] after which they were formed into a parallel beam with a cylinder-aperture lens. The electron current was collected in a cylindrical collector C and measured with an electrometer. The cylinder-aperture lens could be operated either as an accelerating or decelerating lens. Electron beam diameters were about 1 and 3 mm, respectively, due to the different magnifications of the lens. It was not convenient to operate the gun in the accelerating mode below about 100-eV electron energy due to the low beam intensity at low voltages on the Soa lens. Similarly, the high voltages involved prohibited using the decelerating mode above about 500-eV electron energy, so that normally the decelerating mode and accelerating mode were used between 0–175 and 150–1500 eV, respectively. It was demonstrated that the results are not affected by the mode in which the electron gun is operating. A fluorescent screen was used to show that the beam geometry does not change with electron energy in a given mode. Electron current varied with energy, but was usually of the order of 10 μA. Observed proton currents were linear with electron current over more than a decade of electron current, thus indicating negligible trapping of the energetic protons by the space charge in the electron beam. By retarding the electrons at the collector C and recording the derivative of the collected current as a function of retarding voltage the electron energy distribution was found to have about 1-eV half-width. The large size of this measured width may be due in part to the poor retarding geometry.

The scattering chamber and drift region were magnetically shielded so that the maximum fields were about 50 mG, except near the entrance aperature of A where they were somewhat higher. These fields were taken into account in determining the spectrometer focus. Changing the field in A from 0 to 1000 G changed the residual field at the center of the scattering chamber only a few percent. Surfaces of the collision chamber, drift region, magnetic analyzer and exit apertures were gold plated. A large portion of the data was collected with an overlay of Aqua-dag on the gold surface of the collision chamber. The problem of surface potentials is discussed later.

[17] E. A. Soa, *Janaer Jahrbuch 1959* (Carl Zeiss, Jena, 1959), Vol. 1, p. 115; J. A. Simpson, Rev. Sci. Instr. **32**, 1283 (1961).

The 60° sector spectrometer A was designed to focus a parallel beam of ions through the exit slit, E_1, of width 1 mm. The effective radius of curvature of the analyzer when corrected for the effect of fringing fields was 3.37 cm. All other defining apertures (in L_1, L_3, L_4, D, E_2, F) were 3 mm. The calculated resolution of the istrument for a parallel ion beam is then $\Delta E/E=0.1$ where $E+\Delta E$ is the energy which will just not pass through the exit aperture. In agreement with this calculation, measured widths at half maximum of mass peaks of H_2^+ ions accelerated into the mass spectrometer were approximately 10% of the energy of the ions for the range of ion energies 2–100 eV.

The magnetic field needed to focus a singly charged ion of mass M and energy V can be expressed as

$$B=\alpha(MV)^{1/2}, \tag{1}$$

where M is in proton masses and V in eV. The analyzer constant, α, was determined by acceleratiug H_2^+ ions through known voltages and measuring the value of B needed to focus the ions. The energy which the ions have, V, while passing through the spectrometer can be written as

$$V=e(\mathcal{U}+\Delta),$$

where $\mathcal{U}$ is the accelerating voltage and Δ is the contact potential difference between the scattering chamber and the spectrometer. By successively reducing the accelerating voltage the values of the contact potential could be determined using α's computed from V's where Δ is a small part of the total energy. The value of Δ could then be used to correct V and a new α computed. Nineteen determinations gave $\alpha=44.8\pm0.4$. The calculated value of α was $\alpha=42.8$. During an experiment the magnetic fields were determined by measuring the current through the magnet coils. To assure that a given current would give the same magnetic field the magnet was cycled on a standard hysteresis loop. A calibration curve giving magnetic field as a function of coil current was obtained using a Hall-effect probe calibrated against a standard magnet. Magnetic fields during an experiment could be ascertained to within 2%.

Including the uncertainties in the magnet constant and the magnetic field, the ion energies could be determined to within 6%. The error in the energy due to surface potential differences between the scattering chamber and mass analyzer was corrected for by determining the surface potential difference, Δ, as outlined above. The value of Δ varied between 0.02 and 1 V depending on the condition and nature of the surfaces. Aqua-dag surfaces were not systematically better than gold surfaces, but the lowest values of Δ were obtained by using Aqua-dag. Most of the data reported herein were obtained using Aqua-dag surfaces with values of Δ less than 0.1 V.

All data on angular distributions, energy profiles, and relative cross sections of the energetic protons were taken without accelerating or electrostatically focusing

the protons until they were accelerated into the multiplier.[18] Thus, although lenses formed by L_1 L_2 and L_2 L_3 could be used to increase signal strength, they were not used during measurements because it was demonstrated that these lenses could change the observed energy distribution of the protons.

For measurements of relative cross sections for formation of bound H_2^+ the ions were focused into A using lenses L_1 L_2 and L_2 L_3. Since the results within experimental uncertainty were the same when the data were taken at 30° and 90°, it is assumed that the focusing introduced no spurious effects into this determination.

C. Recording and Reduction of Data

The magnetic electron multiplier was run with a gain of between 10^6 and 10^7, measured by integrating the charge associated with individual pulses. Measured output currents from the multiplier were from 10^{-13} to 10^{-10} A, indicating primary ion currents of 10^{-20} to 10^{-16} A. The limiting noise under these conditions was the "shot-noise" in the signal itself. The multiplier output currents were amplified with an electrometer whose output was fed to a data-recording device. For measuring the energy profiles (Exp. 2 outlined in Sec. IIA) the electrometer output was recorded on the ordinate of an $X-Y$ recorder. The abscissa in this case recorded the current in the magnet coils of the spectrometer. When measuring angular distributions and relative cross sections the electrometer output was integrated by an operational amplifier whose output was entered in digital form on punched paper tape. Electron current and energy, magnet current, and angle were also punched on the tape.

To obtain the energy profiles from the $X-Y$ plots of ion current versus magnet current, the noise was averaged by eye to obtain the mean ordinate. The abscissas were converted to magnetic field by a calibration curve as mentioned earlier, and then to energy V from (1). Contact potentials Δ were then subtracted where Δ was greater than 0.1 V.

In reducing the data on angular distributions, the net ion current was normalized to unit electron current then multiplied by $\sin\theta$, where θ as shown in Fig. 2, is the angle between the electron beam and the acceptance axis of the spectrometer. This is necessary since the effective interaction volume (assuming a parallel electron beam and enough collimation in the detector system to give a parallel ion beam) varies geometrically as $1/\sin\theta$. The data were then normalized to unity at 90°.

In determining relative cross sections the ion currents were again normalized to unit electron current, unit pressure, and to standard interaction volume at 90°.

[18] For the measurements of the proton energy profiles a voltage of +10 V was applied to electrode D in order to eliminate the thermal ions from the scans. There was no effect on the profile above 3-eV proton energy.

III. RESULTS AND DISCUSSION

A. Angular Distributions

Of the dissociative collisions of electrons with diatomic molecules (dissociative attachment, dissociative excitation, and dissociative ionization) dissociative ionization is the most difficult[13] to discuss in terms of general symmetry arguments for predicting the angular distribution of products. This is because there are two outgoing electrons whose symmetry properties can be known only by solving the problem in detail. However, several observations about this process can be made.

The matrix element involved in calculating the cross section for such a process is

$$\mathfrak{R}=A\int \exp(i\mathbf{k}\cdot\mathbf{r})\Psi_M V\Psi_I^*\Phi_1^*\Phi_2^* d\tau_e dR, \qquad (2)$$

where $k\hbar$ is the momentum of the incident electron, Ψ_M is the initial wave function of the molecule, Ψ_I is the wave function of the molecular ion formed, Φ_1 and Φ_2 are the wave functions of the outgoing electrons, $d\tau_e$ is the volume element of the electronic coordinates, R is the internuclear separation, A is a constant, and it is assumed that the Coulomb interaction V accounts entirely for the transition. Near the energetic threshold for the process ($k'b\ll 1$ where b, the effective impact parameter, is the order of atomic dimensions, and $k'\hbar$ is the momentum of the scattered electron) the outgoing electrons have zero energy and angular momentum so that both Φ_1 and Φ_2 are spherically symmetric.[19]

At threshold then the selection rules given by Dunn[13] hold exactly, and the transition probability is vanishing or nonvanishing depending on the symmetries of Ψ_M and Ψ_I and upon the initial alignment of the molecule relative to $\mathbf{k}$. For the case at hand the wave function Ψ_M is that of the $^1\Sigma_g^+$ state of H_2 and Ψ_I is that of the $^2\Sigma_u^+$ state of H_2^+. For these states the selection rules dictate a vanishing cross section for initial alignment of the molecule perpendicular to the electron beam and a nonvanishing cross section for parallel alignment.

The dependence on initial alignment is reflected in the angular distribution of dissociation products when Ψ_I is a repulsive state of the molecular ion, since the dissociation normally takes place in a time small compared to the time for one molecular rotation. A simple classical estimate of the angle between the final velocity vector of a dissociating particle and the initial axis of the molecule shows this angle to be

$$\alpha_\infty=(\mathcal{E}_R/\mathcal{E}_S)^{1/2},$$

where $\mathcal{E}_R$ is the energy of rotation and $\mathcal{E}_S$ is the kinetic energy at infinite separation of the dissociating particles. The effect of rotation is to make the angular distribution of products more isotropic. Thus, if the transition

[19] This is, of course, obvious analytically but is also borne out experimentally as in the work of C. B. O. Mohr and F. H. Nicoll, Proc. Roy. Soc. (London) **A144**, 596 (1935).

probability depends as $\cos^2\theta'$, on θ', the angle between $\mathbf{k}$ and the internuclear axis of the molecule, then the angular distribution of products has the dependence, $\cos^2\theta+\mathcal{E}_R/\mathcal{E}_S \sin^2\theta$ when $\mathcal{E}_R/\mathcal{E}_S$ is small. For hydrogen $\mathcal{E}_R$ is of the order 0.02 eV and $\mathcal{E}_S$ is of the order of 1 eV or more for the $^2\Sigma_u^+$ state of H_2^+. In the present experiment, then, the observed relative proton current should be a close representation of the angular dependence of the transition probability.

For electron energies significantly above threshold the wave functions Φ_1 and Φ_2 in (2) are no longer necessarily spherically symmetric. They are rather complicated functions, and it is difficult to say anything general about their symmetries without solving the problem in detail.

It seems reasonable, however, to make some estimates by analogy with the less complicated process of dissociative excitation. In order to conserve momentum in an ionizing collision at electron energies significantly above threshold the most probable direction for the momentum of the ejected electron is opposite that of the momentum change vector of the scattered electron. This direction then defines a symmetry axis in analogy to dissociative excitation. For high energies the transition probability is dominated[13,20] by the term, $|\mathbf{K}\cdot\langle\mathbf{M}\rangle|^2$, where $\langle\mathbf{M}\rangle$ is the dipole matrix element for the transition being considered and $\mathbf{K}$ is the momentum change vector $\mathbf{k}'-\mathbf{k}$ of the scattered electron.

Zare and Herschbach[21] have discussed in detail the geometrical transformation of the expression $|\mathbf{K}\cdot\langle\mathbf{M}\rangle|^2$ to a laboratory fixed system. Applying their transformation to the present case of a $\Sigma_g^+\rightarrow\Sigma_u^+$ transition the angular distribution should be given by

$$I_\theta(E,\epsilon)=\mathrm{B}[\cos^2\eta(E,\epsilon)\cos^2\theta+(1/2)\sin^2\eta(E,\epsilon)\sin^2\theta], \quad (3)$$

where η is the angle between $\mathbf{K}$ and $\mathbf{k}$, θ is the angle between $\mathbf{k}$ and the axis along which observations are made, and B depends on electron energy but not on angle. As η increases from small values the angular distribution becomes increasingly isotropic. At $\eta=54.7°$ the distribution is isotropic, and for larger values of η the distribution has its maximum at right angles to the electron beam. This picture fits smoothly into the picture at threshold, although, the $|\mathbf{K}\cdot\langle\mathbf{M}\rangle|^2$ term is not dominant there.

The observed angular distributions of 8.6-eV protons are shown in Fig. 3. The qualitative features of the expected angular distributions are verified. At energies close to threshold the protons are very strongly peaked along the electron beam. As the electron energy goes up the angular distribution becomes more isotropic.

There is a systematic difference between the magnitude of the proton signals observed in the forward quadrants and those observed in the backward quadrants. This difference appears to be connected with the fact that the scattering chamber is not symmetric forward-backward (Fig. 2). Due to space limitations the electron gun extends into the scattering chamber. The angular distribution of thermal H_2^+ ions was observed to be isotropic, as expected, in the forward quadrants but not in the backward quadrants. This result implies that the angular distributions of fast protons observed in the forward quadrants are representative of the backward quadrants also. This was assumed in the analysis of the data.

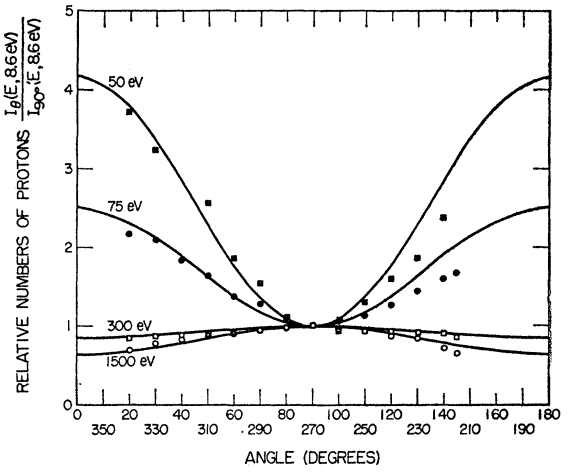

FIG. 3. Angular distribution of 8.6-eV protons for various electron energies. Data taken at angles symmetric to the electron beam axis (left-right) have been averaged as indicated by the abscissa. All of the data have been corrected for the variation of scattering volume with angle by multiplying by $|\sin\theta|$ and then normalized by making the average of the proton current observed at 90° and 270° equal to 1.0. The solid curves are fits of (5) to the data taken at forward angles. The data taken at backward angles are systematically lower than those taken at forward angles. This effect appears to be associated with the lack of forward-backward symmetry in the scattering chamber. This asymmetry is discussed further in the text.

The discussion of these results may be put in more quantitative terms by using a quantity to be called the polarization $P(E,\epsilon)$ which is defined by the equation

$$P(E,\epsilon)=2\cot^2\eta(E,\epsilon)-1. \quad (4)$$

Then, (3) becomes

$$I_\theta(E,\epsilon)=I_{90°}(E,\epsilon)[1+P(E,\epsilon)\cos^2\theta]. \quad (5)$$

This is a form often encountered for dipole transition processes. The solid curves in Fig. 3 show how (5) represents the data when values of $P(E,\epsilon)$ are chosen empirically.

The measured angular distributions were used to compute $P(E,\epsilon)$ from (5) for those electron energies and proton energies at which measurements were made. Figure 4 shows $P(E,\epsilon)$, plotted as a function of electron energy E, for three values of proton energy ϵ. The dashed vertical lines indicate the electron energy thresholds for production of protons having these three proton energies. One sees how rapidly the angular

[20] H. S. W. Massey, in *Encyclopedia of Physics*, edited by S. Flügge (Springer-Verlag, Berlin, 1956), Vol. 36, p. 356.
[21] R. N. Zare and D. R. Herschbach, Proc. IEEE **51**, 173 (1963).

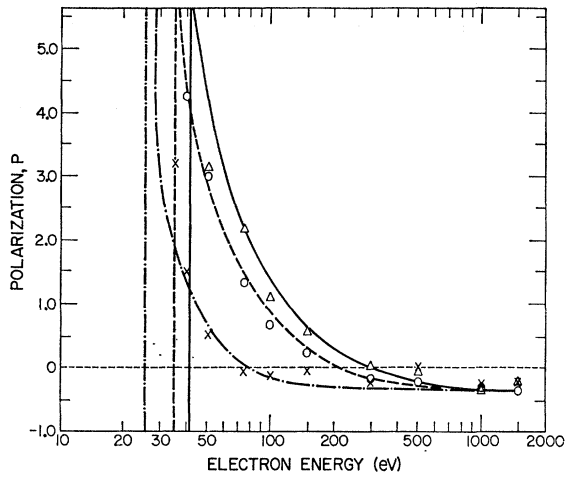

FIG. 4. Polarization P as a function of electron energy for three proton energies. P is defined by (5). The solid curve is a fit to the triangular data points for 11.8-eV protons; the dashed curve is a fit to the circular data points for 8.6-eV protons; and the dot-dash curve is a fit to the cross data points for 3.7-eV protons. The vertical lines on the diagram are drawn at the electron energy for the appearance of protons whose energy is indicated by the designation of energies of the fitted curves. The appearance potentials used were determined from Fig. 1 assuming that the protons observed were from the $^2\Sigma_u^+$ dissociative state of H_2^+.

distributions become isotropic as the electron energy increases above the thresholds.

If the dipole analogy has meaning then the experimental data can be used in (4) to obtain η. Figure 5 shows η as a function of E for the same three values of ϵ. Dashed vertical lines show the thresholds as in Fig. 4. The figure shows that an asymptotic limit of about 60° is obtained for η. Although a detailed comparison cannot be made, the results of Mohr and Nicoll[19] imply a preferred angle, near 60°, for electrons ejected from H_2 in ionization by electron impact.

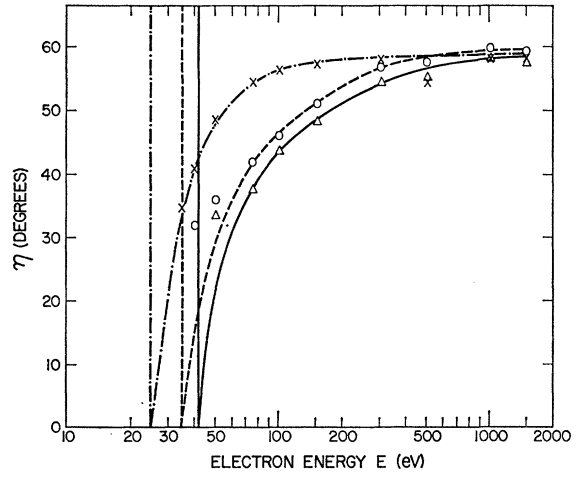

FIG. 5. The angle η as a function of electron-impact energy. η is the angle between the momentum vector of the impacting electron and its momentum-change vector. The points plotted here were obtained by solving (4) for η, using values of P from Fig. 4. The curves were sketched in to give the general trend of the data. The diamonds and solid curve are for 11.8-eV protons; the circles and dashed curve are for 8.6-eV protons; and the crosses and dot-dash curve are for 3.7-eV protons. The appearance potentials for the various energy ions are indicated by the corresponding vertical lines.

B. Proton Energy Distributions

In the repulsive $^2\Sigma_u^+$ electronic state of H_2^+ there is a continuum of states for the nuclear motion. A transition to a particular state in this continuum will result in a dissociating atom and proton with unique kinetic energies. As the transition probability to different final states in the continuum varies, this should be observed as a corresponding variation in the proton energy distribution.

In the usual discussion of the Franck-Condon principle[22] one assumes that it is a good approximation to write the molecular wave functions as a product of electronic and nuclear wave functions, neglecting the rotation, so that

$$\Psi_M=\psi_{eM}\chi_v$$

and

$$\Psi_I=\psi_{eI}\chi_\nu$$

where χ_v indicates the discrete vibrational state of Ψ_M, χ_ν the continuum state of Ψ_I, and ψ_{eM} and ψ_{eI} are the electronic wave functions of the molecule and ion, respectively. χ_v and χ_ν depend only on the internuclear separation R.

When ψ_{eM} and ψ_{eI} are combined with the incoming and outgoing electron waves, respectively, to give ϕ_{eM} and ϕ_{eI}, (2) becomes

$$\mathfrak{R}=A\int\phi_{eM}V\phi_{eI}^*\chi_\nu^*\chi_v d\tau_e d\tau_N.$$

Carrying out the integration over electronic coordinates, this becomes

$$\mathfrak{R}=A\int U_N\chi_v\chi_\nu^* d\tau_N.$$

The assumption of the Franck-Condon principle is that U_N is nearly constant over the small range of R at which χ_v has appreciable values, and may be taken out of the integral, so that

$$\mathfrak{R}=A\bar{U}_N\int\chi_v\chi_\nu^* d\tau_N=A\bar{U}_N\mathcal{O}_{v\nu}.$$

Since the cross section is proportional to $|\mathfrak{R}|^2$ this says that the cross section is proportional to the square of the overlap integral $\mathcal{O}_{v\nu}^2$ of the initial and final internuclear (or vibrational) wave functions,

$$\sigma\propto A^2\bar{U}^2\mathcal{O}_{v\nu}^2. \quad (6)$$

[22] G. Herzberg, *Spectra of Diatomic Molecules* (D. Van Nostrand Company, Inc., Princeton, New Jersey, 1950), p. 199; J. Franck, Trans. Faraday Soc. **21**, 536 (1925); E. U. Condon, Phys. Rev. **28**, 1182 (1926).

For ionizing collisions the cross section varies linearly[23] with excess electron energy above threshold for some energy range. The cross section can then be written

$$\sigma = G(E-E_T)\mathcal{O}_{v\nu}^2 = G(E-E_0-\epsilon_A-\epsilon_B)\mathcal{O}_{v\nu}^2, \quad (7)$$

where E_0 is the threshold energy for producing ions of zero kinetic energy, ϵ_A and ϵ_B are the kinetic energies of the dissociating particles **A** and **B**, respectively, and G is a constant. For H_2, $\epsilon_A=\epsilon_B=\epsilon$. Also each state ν corresponds to a unique kinetic energy ϵ so that (7) can as well be rewritten

$$\sigma = G(E-E_0-2\epsilon)\mathcal{O}_{v\epsilon}^2. \quad (8)$$

Thus σ depends on ϵ both through $\mathcal{O}_{v\epsilon}^2$ and the quantity in parentheses.

The linear dependence on energy above threshold of the electronic part of the cross section is valid only for some small energy range. However, it is a reasonable approximation up to electron energies the order of 70 eV (see Fig. 10). When the electron energy is this high the fractional difference in the electronic part of the cross section for transitions yielding different energies ϵ is quite small. So at high electron energies the distribution in ion kinetic energies is determined almost entirely by $\mathcal{O}_{v\epsilon}^2$.

Evaluation of $\mathcal{O}_{v\epsilon}^2$ requires knowledge of χ_v and χ_ν. Several approximate methods have been reported. The so-called "reflection approximation"[5] is used in the following discussion. This assumes that χ_ν can be replaced with an appropriately normalized δ function at the classical turning point, i.e., $\chi_\nu = S\delta(R-R_1)$. In this case,

$$\mathcal{O}_{v\epsilon}^2 = S^2|\chi_v(R_1(\epsilon))|^2, \quad (9)$$

since each R_1 corresponds to a unique value of ϵ. R_1 is the value of R at which the internuclear potential energy for the final state is equal to 2ϵ and S is a normalization constant.

The method suggested by Collidge, James, and Present[24] has been employed to normalize the δ functions used for χ_ν. The potential energy curves for H_2^+ given by Bates, Ledsham, and Stewart,[25] and the harmonic oscillator function with constants quoted by Stevenson[6] for $\chi_v(R)$ were used in the calculations. The results for $\mathcal{O}_{v\epsilon}^2$ are shown in the left-hand insert of Fig. 1.

The solid line in Fig. 6 shows the proton energy distribution as measured in this experiment for 75 eV electrons; the dashed curve is the result of the calculation just described taking the $^2\Sigma_u^+$ state of H_2^+ as the final state; and the dot-dash curve shows the measurement of Lozier[2] at the same electron energy. The latter measurement is typical of several such reported in the literature.[3-6] Stevenson[6] has pointed out the disagreement of these measurements with the predictions of the Franck-Condon principle and has speculated about physical processes which might account for the disagreement. The present results agree quite satisfactorily with present calculations so that such speculation seems unnecessary.

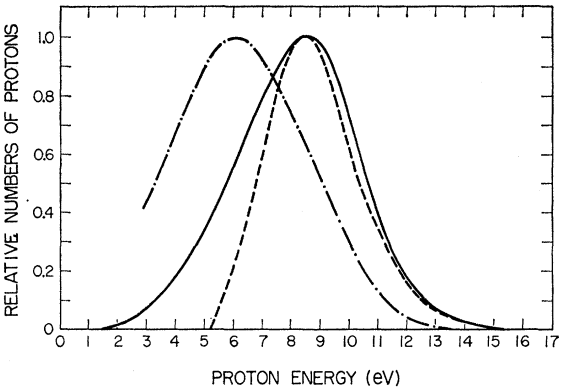

FIG. 6. The energy distribution of protons from the dissociative ionization of H_2. The dashed curve was calculated using the Franck-Condon principle assuming the transition involved was from the ground state of H_2 to the $^2\Sigma_u^+$ state of H_2^+. Normalized delta functions were used for the H_2^+ internuclear wave functions. The solid curve was measured in this experiment for 75-eV electrons. The dot-dash curve is a measurement of Lozier which is typical of previous results reported in the literature.

One does note that the experimental results show more ions at energies below 8 eV than expected from the calculation. The use of δ functions for χ_ν will be an increasingly worse approximation at large internuclear separations. This would tend to deemphasize ions of lower kinetic energies in the calculation. Also in this calculation no account has been taken of possible contributions of ions from excited states of H_2^+; although as stated earlier, it is not expected these states will contribute appreciable numbers of ions.

As noted previously,[10] ions with energies below 1.5 eV were excluded from the detector. Thus, in Fig. 6 protons from the $^2\Sigma_g^+$ state are not shown. These ions can only be well separated from the thermal H_2^+ ions by acceleration. They were readily observed under these conditions.

The details of the present experiment are in Sec. II, but it is emphasized again at this point that no electrostatic fields were employed in the energy measurements reported here that would give rise to an energy dispersion of a complicated nature to affect the results.

At lower electron energies the quantity in parentheses in (8) contributes significantly to the expected proton energy distribution. The position of the maximum of the proton energy distribution as a function of E can be predicted simply by equating the derivative of the function in (8) to zero and finding the root ϵ for various E. The position of the peak ϵ_{max} is plotted as a function of electron energy E in Fig. 7. Results of this and previous experiments are also shown in the figure; the present results are in significantly better agreement with

[23] S. Geltman, Phys. Rev. **102**, 171 (1956).
[24] A. S. Coolidge, H. M. James, and R. D. Present, J. Chem. Phys. 4, 193 (1936).
[25] D. R. Bates, K. Ledsham, and A. L. Stewart, Phil. Trans. Roy. Soc. (London) **A246**, 215 (1953).

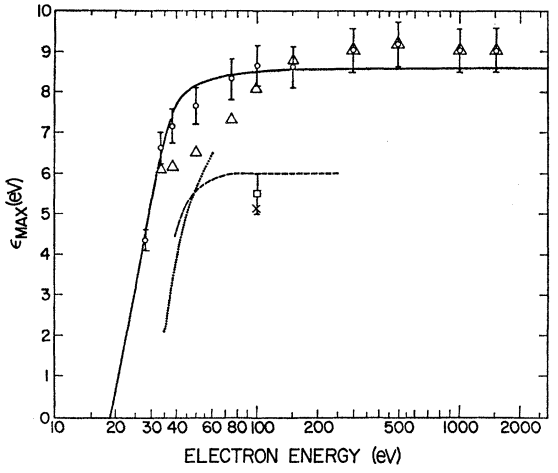

FIG. 7. The energy at which the proton-energy distribution has its maximum as a function of electron energy. The solid curve was calculated by maximizing the cross section given by (8) with respect to ϵ assuming an isotropic distribution of protons (ϵ designates the proton energy). The circles are data taken in this experiment at 30° and 40°. The triangles are data taken in this experiment at 90°. The dashed curve is Lozier's data, and the dotted curve is Newhall's. The square is due to Stevenson, and the cross to Hagstrum, and Hagstrum and Tate.

the predictions outlined above than previously reported results.

The points in Fig. 7 obtained at 90° are systematically below the predicted values and below the points obtained at 30° and 40° for electron energies below about 100 eV. This is particularly noticeable near the "knee" of the curve.

It can be shown that for an angular distribution of the form given by (5), and for a total cross section given by (8), the intensity of ions observed at an angle θ is

$$I_\theta(E,\epsilon)=\frac{C(E-E_0-2\epsilon)}{D_\theta(E,\epsilon)}\mathcal{O}_{v\epsilon}{}^2, \tag{10}$$

where C is a scaling constant,

$$D_\theta(E,\epsilon)=\frac{1+[P(E,\epsilon)/3]}{1+P(E,\epsilon)\cos^2\theta}, \tag{11}$$

and other term have been previously defined.

It is easily seen from (11) that at 54.7° (i.e., for $\cos^2\theta=\frac{1}{3}$) the observed intensity is independent of polarization. At this angle, then, one observes the energy distributions characteristic of the total cross section in (8).

By fitting the data in Fig. 4 an approximate functional form for $P(E,\epsilon)$ was obtained. This has been used in (10) to find ϵ such that $I_\theta(E,\epsilon)$ is a maximum. Fig. 8 shows $\epsilon_{\max 90°}/\epsilon_{\max 54.7°}$ and $\epsilon_{\max 30°}/\epsilon_{\max 54.7°}$ as a function of electron energy. This shows that in qualitative agreement with the data in Fig. 7 the points at 90° are systematically below those at 30°, with the percentage difference (except for the very large differences near threshold) being largest near the knee of the curve. It is striking, however, to note that the percent difference is less than 3 or 4% except at electron energies below 25 V, for which the difference rapidly becomes very large.

C. Relative Cross Sections

The total cross section for production of protons of a given energy from dissociative ionization is related to the intensity observed at angle θ by

$$\sigma(E,\epsilon)=F\int_0^\pi I_\theta(E,\epsilon)2\pi\sin\theta d\theta, \tag{12}$$

where F is a constant which includes collection efficiency, scaling factors, etc. When $I_\theta(E,\epsilon)$ is substituted from (5) and the indicated integration carried out

$$\sigma(E,\epsilon)=\left[\frac{4\pi}{3}\right]F[3+P(E,\epsilon)]I_{90°}(E,\epsilon); \tag{13}$$

and using (5) and (11)

$$\sigma(E,\epsilon)=[4\pi F]D_\theta(E,\epsilon)I_\theta(E,\epsilon). \tag{14}$$

At $\theta=54.7°$ the cross section is directly proportional to the observed intensity of protons. At other angles, however, the observed intensity must be multiplied by a correction factor $D_\theta(E,\epsilon)$ to obtain the correct form for the total cross section. This factor is shown in Fig. 9 for 8.6-eV protons as a function of energy for three values of θ.

The proton yield as a function of electron energy was measured at three angles for 8.6-eV protons. These results are shown in Fig. 10. The curves for 90° and 54.7° are deduced using $D_\theta(E,\epsilon)$ shown in Fig. 8 and the measured proton intensity at 30°.

These results demonstrate the large effect which the anisotropy in proton angular distributions can have on

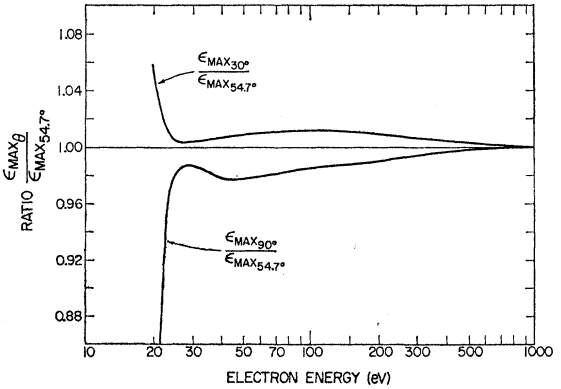

FIG. 8. Ratio of the energy at which the peak of the proton energy distribution should occur for observations at 30° and 90° to the energy of the peak of the proton energy distribution observed at 54.7° as a function of electron energy. The $\epsilon_{\max\theta}$ were obtained by maximizing $I_\theta(E,\epsilon)$ as given by (10) with respect to ϵ. This is in qualitative agreement with the data presented in Fig. 7.

the shape and magnitude of the cross section curve for a specific proton energy.

The relative cross section for formation of H_2^+ was measured to test the reliability of this instrument for determining relative cross sections. Satisfactory agreement of shape with Tate and Smith's[26] results were obtained over the energy range covered by their experiments.

The ratio of proton current to H_2^+ current was observed. However, because of difficulties such as an uncertainty in the relative efficiency of the multiplier for the two ions, no attempt was made to make a definitive measurement of this ratio. Ignoring such difficulties the ratio observed was of the order of 10% in reasonable agreement with Bleakney's value of 8%.[1]

IV. CONCLUSIONS

The anisotropy in the angular distribution of protons from dissociative ionization of H_2 has been observed to be a strong function of electron energy over the range from threshold to 1500 eV. The anisotropy near threshold is consistent with predictions of Dunn.[13] Analysis of the angular distributions over the entire energy range in terms of a dipole transition is consistent with all of our observations and with the observations of electron scattering by Mohr and Nicoll.[19]

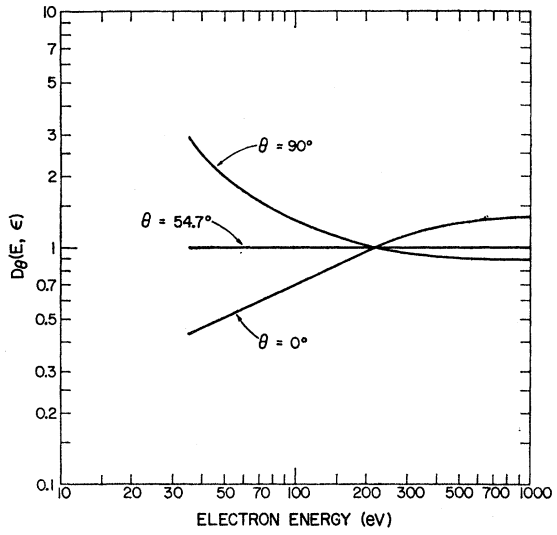

FIG. 9. $D_\theta(E,\epsilon)$ defined by (11) as a function of electron energy for $\epsilon=8.6$ eV. The curves are obtained from (11) using values of $P(E,\epsilon)$ from Fig. 4.

[26] J. T. Tate and P. T. Smith, Phys. Rev. **39**, 270 (1932).

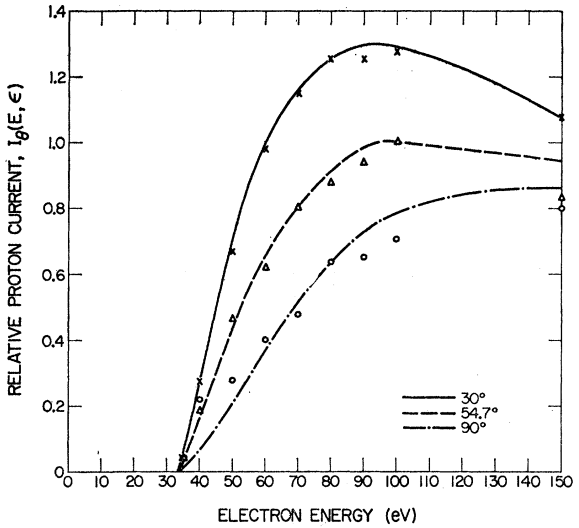

FIG. 10. Relative proton current, $I_\theta(E,\epsilon)$ for $\epsilon=8.6$ eV as a function of electron energy E. The curves were determined by fitting a curve to the data taken at 30° (crosses). The shape of the total relative cross section, given by Eq. (14), was then determined from the fitted curve using $I_{30°}$ (E, 8.6 eV), and $D_{30°}$ (E, 8.6 eV). This fitted cross-section curve was then used to obtain I_θ (E, 8.6 eV) for the three angles indicated.

It has been shown that anisotropies such as observed here can have a significant effect on measurements of such quantities as cross sections and energy distributions of dissociation products.

The energy distributions of protons measured in this experiment are in good agreement with predictions of the Franck-Condon rule over the entire energy range of observation. It can only be conjectured that the difference of our result with the results of other workers arises because of the very different measurement technique.

ACKNOWLEDGMENTS

The authors achnowledge the help of J. Arol Simpson and C. E. Kuyatt of the Electron Physics Section of the National Bureau of Standards for design of the electron gun used. They also acknowledge stimulating discussions with their colleagues in JILA.